







Article

Evaluation of the Preclinical Efficacy of Lurbinectedin in Malignant Pleural Mesothelioma

Dario P. Anobile ^{1,†}, Paolo Bironzo ^{1,2,†}, Francesca Picca ^{1,3}, Marcello F. Lingua ⁴, Deborah Morena ^{1,3}, Luisella Righi ^{1,5}, Francesca Napoli ^{1,5}, Mauro G. Papotti ^{1,6,7}, Alessandra Pittaro ^{1,6} , Federica Di Nicolantonio ^{1,8} , Chiara Gigliotti ^{1,8}, Federico Bussolino ^{1,7,8}, Valentina Comunanza ^{1,8} , Francesco Guerrera ^{9,10} , Alberto Sandri ¹¹, Francesco Leo ^{1,11}, Roberta Libener ¹², Pablo Aviles ¹³, Silvia Novello ^{1,2}, Riccardo Tauli ^{1,3}, Giorgio V. Scagliotti ^{1,2,7,*}  and Chiara Riganti ^{1,7,14,*} 

¹ Department of Oncology, University of Torino, 10043 Orbassano, Italy; dario.anobile@edu.unito.it (D.P.A.); paolo.bironzo@unito.it (P.B.); francesca.picca@unito.it (F.P.); deborah.morena@unito.it (D.M.); luisella.righi@unito.it (L.R.); francesca.napoli@unito.it (F.N.); mauro.papotti@unito.it (M.G.P.); apittaro@cittadellasalute.to.it (A.P.); federica.dinicolantonio@unito.it (F.D.N.); chiara.gigliotti@unito.it (C.G.); federico.bussolino@unito.it (F.B.); valentina.comunanza@unito.it (V.C.); francesco.leo@unito.it (F.L.); silvia.novello@unito.it (S.N.); riccardo.tauli@unito.it (R.T.)

² Thoracic Unit and Medical Oncology Division, Department of Oncology at San Luigi Hospital, University of Torino, 10043 Orbassano, Italy

³ Center for Experimental Research and Medical Studies (CeRMS), City of Health and Science University Hospital di Torino, University of Torino, 10126 Torino, Italy

⁴ Department of Medical Sciences, University of Torino, 10126 Torino, Italy; marcello.lingua@edu.unito.it

⁵ Pathology Unit, San Luigi Hospital, University of Torino, 10043 Orbassano, Italy

⁶ Pathology Unit, City of Health and Science University Hospital, 10126 Torino, Italy

⁷ Interdepartmental Centre for Studies on Asbestos and Other Toxic Particulates, University of Torino, 10125 Torino, Italy

⁸ Candiolo Cancer Institute—FPO, IRCCS, 10060 Candiolo, Italy

⁹ Department of Surgical Science, University of Torino, 10126 Torino, Italy; francesco.guerrera@unito.it

¹⁰ Department of Thoracic Surgery, City of Health and Science University Hospital, 10126 Torino, Italy

¹¹ Thoracic Surgery Division, San Luigi Hospital, University of Torino, 10043 Orbassano, Italy;

al.sandri@sanluigi.piemonte.it

¹² Department of Integrated Activities Research and Innovation, Azienda Ospedaliera SS. Antonio e Biagio e Cesare Arrigo, 15121 Alessandria, Italy; rlibener@ospedale.al.it

¹³ Research and Development Department, PharmaMar, 28770 Colmenar Viejo, Madrid, Spain; paviles@pharmamar.com

¹⁴ Interdepartmental Research Center of Molecular Biotechnology, University of Torino, 10126 Torino, Italy

* Correspondence: giorgio.scagliotti@unito.it (G.V.S.); chiara.riganti@unito.it (C.R.)

† These authors contributed equally to this work.



Citation: Anobile, D.P.; Bironzo, P.; Picca, F.; Lingua, M.F.; Morena, D.; Righi, L.; Napoli, F.; Papotti, M.G.; Pittaro, A.; Di Nicolantonio, F.; et al. Evaluation of the Preclinical Efficacy of Lurbinectedin in Malignant Pleural Mesothelioma. *Cancers* **2021**, *13*, 2332. <https://doi.org/10.3390/cancers13102332>

Academic Editor: Daniel L. Pouliquen

Received: 20 April 2021

Accepted: 10 May 2021

Published: 12 May 2021

Publisher's Note: MDPI stays neutral with regard to jurisdictional claims in published maps and institutional affiliations.



Copyright: © 2021 by the authors. Licensee MDPI, Basel, Switzerland. This article is an open access article distributed under the terms and conditions of the Creative Commons Attribution (CC BY) license (<https://creativecommons.org/licenses/by/4.0/>).

Simple Summary: The marine drug lurbinectedin revealed an unprecedented efficacy against patient-derived malignant pleural mesothelioma cells, regardless of the histological type and the BAP1 mutation status. By inducing strong DNA damages, it dramatically arrested cell cycle progression and induced apoptosis. These results may be translated into the use of lurbinectedin as an effective agent for malignant pleural mesothelioma patients.

Abstract: Background: Malignant pleural mesothelioma (MPM) is a highly aggressive cancer generally diagnosed at an advanced stage and characterized by a poor prognosis. The absence of alterations in druggable kinases, together with an immune-suppressive tumor microenvironment, limits the use of molecular targeted therapies, making the treatment of MPM particularly challenging. Here we investigated the in vitro susceptibility of MPM to lurbinectedin (PM01183), a marine-derived drug that recently received accelerated approval by the FDA for the treatment of patients with metastatic small cell lung cancer with disease progression on or after platinum-based chemotherapy. Methods: A panel of primary MPM cultures, resembling the three major MPM histological subtypes (epithelioid, sarcomatoid, and biphasic), was characterized in terms of BAP1 status and histological markers. Subsequently, we explored the effects of lurbinectedin at nanomolar concentration on cell cycle, cell viability, DNA damage, genotoxic stress response, and proliferation. Results: Stabilized

MPM cultures exhibited high sensitivity to lurbinectedin independently from the BAP1 mutational status and histological classification. Specifically, we observed that lurbinectedin rapidly promoted a cell cycle arrest in the S-phase and the activation of the DNA damage response, two conditions that invariably resulted in an irreversible DNA fragmentation, together with strong apoptotic cell death. Moreover, the analysis of long-term treatment indicated that lurbinectedin severely impacts MPM transforming abilities in vitro. Conclusion: Overall, our data provide evidence that lurbinectedin exerts a potent antitumoral activity on primary MPM cells, independently from both the histological subtype and BAP1 alteration, suggesting its potential activity in the treatment of MPM patients.

Keywords: MPM; lurbinectedin; DNA damage response

1. Introduction

Malignant pleural mesothelioma (MPM) is a rare but extremely aggressive type of cancer arising from pleural mesothelium and is highly associated with asbestos exposure. The disease is characterized by a long latency between initial exposure to asbestos and the clinical onset of the disease (30–50 years) and, although in Western regions the peak was expected in the 2020s [1], the ongoing use of asbestos in developing countries could lead to a persistence of new cases in the next decades [2]. MPM is classified into three major histological subtypes: epithelioid, sarcomatoid, and biphasic. While the epithelioid subtype occurs more frequently, accounting for approximately 60% of cases, and correlates with a better outcome, the sarcomatoid subgroup represents 10–20% of the cases and is characterized by a worse prognosis [3,4]. Independently from the morphology, the MPM tumor microenvironment is particularly enriched of immunosuppressive cells, which makes this tumor particularly refractory to different therapies [5–10]. Moreover, MPM is generally diagnosed in advanced stage, minimizing the role of curative treatments. For advanced-stage disease, the first-line systemic treatment consists of cisplatin and pemetrexed [11], a combination that prolongs the median survival time of only 3 months. Recently, the combination of immune checkpoint inhibitors directed against programmed death-1 (PD-1) and cytotoxic-T-lymphocyte-associated protein 4 (CTLA-4) showed its superiority over chemotherapy in previously untreated and unresectable MPM, especially in non-epithelioid tumors [12]. Conversely, no second-line standard therapy has been approved, despite the pre-clinical and the clinical evaluation of different therapeutic agents [13,14].

The genomic landscape of MPM reveals a low mutational burden with inactivating alterations mainly on oncosuppressors (BAP1, CDKN2A, NF2, TP53, LATS2, and SETD2) [15–18] thus precluding the use of molecular therapies against activated oncogenes. Among the oncosuppressors, BAP1 (BRCA1-associated protein) alterations account from 30% to 60% of cases [15,17,19,20]. Indeed, BAP1 germline mutations are known to predispose to mesothelioma and other cancer-associated syndromes [21,22] thus indicating a critical role for this deubiquitinase in suppressing tumor development. BAP1 regulates different biological processes among which chromatin modification, cell cycle, apoptosis, ferroptosis, cell metabolism, and differentiation [23]. Notably, BAP1 is involved in DNA synthesis, DNA duplication under stress conditions [24,25], and DNA damage response, by modulating the function of the BRCA1/BARD1 (BRCA1 Associated RING Domain 1) complex and coordinating the recruitment of RAD51 to the damaged DNA loci [26,27].

Lurbinectedin (PM01183) is a marine-derived anticancer drug that exerts a potent antitumor activity in different cancer cell lines and xenografts models and is currently under clinical evaluation in several tumor types [28–35]. Recently, the FDA has released a conditional approval for lurbinectedin for the treatment of second-line metastatic small cell lung cancer patients [36] while promising antitumor activity has been reported in MPM patients in second- and third-line [37]. However, there are no data available on the role of lurbinectedin as monotherapy or in combination in the first-line treatment of MPM. At

the molecular level, lurbinectedin covalently binds CG-rich sequences in the DNA minor groove. The presence of the drug on the DNA helix inhibits the transcriptional process and is associated with the generation of DNA breaks [28]. Moreover, the interaction of lurbinectedin with both DNA strand breaks also interferes with the enzymes involved in the DNA damage response [38].

Here, we report about the potential efficacy of lurbinectedin in a panel of primary MPM cultures. Specifically, we demonstrated that lurbinectedin is strongly effective at nanomolar concentration and interferes with the transforming properties of MPM in a way that is independent of the BAP1 status and histological classification. With the caveat that our cell cultures were derived from diagnostic biopsies or surgical resections, our data indicate that lurbinectedin could potentially be explored in the management of patients with advanced MPM as second-line treatment or part of combination treatment in first-line.

2. Results

2.1. Primary Mesothelioma Cell Cultures Characterization

Twelve primary MPM cell lines, derived from patients with different histology, were stabilized as 2D cultures (Figure 1A). Flow cytometry for pan-cytokeratin (Figure 1B), immunohistochemical analysis (Figure 1C and Table 1), and immunoblotting for the BAP1 status (Figure 1D) were used to characterize the MPM cell lines. Notably, our panel (6 BAP1+ and 6 BAP1– cultures) was representative of the three major MPM histological subtypes (epithelioid, sarcomatoid, and biphasic) (Table S1).

Table 1. Histological characterization of MPM cultures.

UPN	BAP1	Pan-CK	WT1	CALR
1	POS	POS	POS	POS
2	POS	POS	NEG	NEG
3	POS	POS	POS	NEG
4	POS	POS	POS	POS
5	POS	NEG	POS	POS
6	POS	POS	NEG	NEG
7	NEG	POS	POS	POS
8	NEG	POS	POS	NEG
9	NEG	POS	POS	POS
10	NEG	POS	POS	POS
11	NEG	POS	NEG	POS
12	NEG	POS	NEG	NEG

Results of the immunohistochemical stainings of MPM samples for BRCA1 associated protein-1 (BAP1), pancytokeratin (pan-CK), Wilms tumor-1 antigen (WT1), calretinin (CALR). POS: positive; NEG: negative.

2.2. Lurbinectedin Exerts Anti-Proliferative Effects in Patient-Derived Mesothelioma Cells

As shown in Figure 2, lurbinectedin decreased the viability of MPM cells in a dose-dependent manner, with an IC₅₀ in the low nanomolar range for all cell lines (Table 2), independently from the BAP1 status and the histological subtype (Figure 2A–D). Indeed, although the IC₅₀ was slightly higher in BAP1– vs. BAP1+ cells (Figure 2C) as well as in the sarcomatoid/biphasic vs epithelioid histotype (Figure 2D), the difference was not statistically significant. Notably, UPN6, UPN10, and UPN12 received trabectedin as second-line treatment and their overall survival was <12 months (Table S1). The cell lines derived from these patients had indeed the highest IC₅₀ in the panel analyzed, but it was below 5 nM for all of them (Table 2).

2.3. Long-Term Lurbinectedin Treatment Impacts on MPM Transforming Abilities

Since mesothelioma is particularly resistant to conventional chemotherapy, we evaluated the long-term effect of lurbinectedin in terms of inhibiting cell proliferation by

performing a crystal violet viability assay. Also in this setting, nanomolar concentrations of lurbinectedin dramatically reduced cell growth (Figure 3A,B). Furthermore, we extended our analysis by testing lurbinectedin ability to interfere with the anchorage-independent growth of MPM cells. The number of visible colonies was markedly decreased upon treatment, showing long-term anticancer efficacy (Figure 3C,D). Importantly, the consistent reduction in anchorage-independent growth showed no differences between BAP1+ and BAP1− cells, suggesting that lurbinectedin strongly impairs the tumorigenic potential of MPM cells, independently from the BAP1 status.

Table 2. IC₅₀ values of MPM cell lines treated with lurbinectedin.

UPN	IC ₅₀ L (nM)
1	0.073
2	0.33
3	0.28
4	0.35
5	1.09
6	1.13
7	0.085
8	0.65
9	0.23
10	3.29
11	0.76
12	4.54

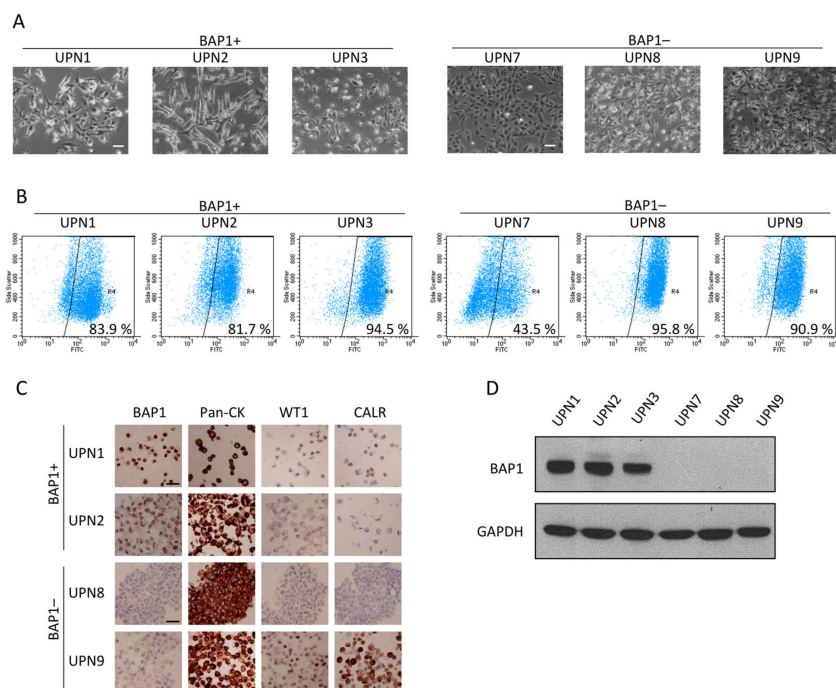


Figure 1. Characterization of patient-derived MPM cell lines. (A) Representative images showing different morphology of three BAP1 positive (BAP1+) and three BAP1 negative (BAP1−) MPM cell lines (scale bar = 100 μ m). (B) Flow cytometry plot representing the percentage of pancytokeratine positive cells in the indicated MPM cell lines. (C) Immunohistochemical analysis of BAP1, pan-cytokeratin (pan-CK), Wilms tumor-1 antigen (WT1), and calretinin (CALR) in the indicated MPM cell lines (scale bar = 100 μ m). (D) Western blot analysis showing BAP1 status of the reported MPM cell lines.

2.4. Lurbinectedin Treatment Interferes with Cell Cycle Progression

To study the molecular basis of this anti-proliferative activity, we analyzed the effect of lurbinectedin on cell cycle regulation. While we observed variable changes in the percentage of cells in the G2/M-phase, indicating an unlikely strong mitotic arrest, we observed a constant accumulation of cells in the S-phase (Figure 4 and Supplementary Figure S1). This event occurred in both BAP1+ and BAP1– cells, suggesting that lurbinectedin-mediated perturbation of the cell cycle is BAP1-independent.

2.5. Lurbinectedin Induces a Profound DNA Damage Coupled with Strong Apoptosis

Among the pleiotropic mechanisms of action of lurbinectedin [28,38] the increase of S-phase arrested cells is suggestive of irreversible DNA damage. Indeed, lurbinectedin induced a significant increase in round-shaped and dense cells (Supplementary Figure S2). The presence of irreversible DNA fragmentation was evaluated by the Single Cell Gel Electrophoresis (SCGE). Specifically, in both BAP1+ and BAP1– cells lurbinectedin induced a dose-dependent genomic fragmentation (Figure 5A,B). The presence of genotoxic stress was confirmed by the increase in the phospho (Ser345) Chk1 and phospho (Thr68) Chk2 (Figure 5C,D), two cell cycle checkpoints that block DNA replication after being phosphorylated by the DNA-damaging sensors ATM/ATR kinases [39]. Moreover, in lurbinectedin-treated cells, we observed the accumulation of phospho (Ser15) p53 and phospho (Ser139) H2AX (Figure 5C,D), two additional targets of ATM/ATR kinases that are generally phosphorylated in response to DNA strand breaks and stalled replication [40,41]. This provided additional evidence of the strong DNA damage induced by lurbinectedin, which is also responsible for cell growth arrest (Figure 4 and Supplementary Figure S1). Such mitotic catastrophe is often coupled with apoptosis [40]. Accordingly, lurbinectedin treatment resulted in a strong induction of apoptosis (Figure 6A,B) as also shown by the dose-dependent activation of caspase 3 (Figure 6C,D).

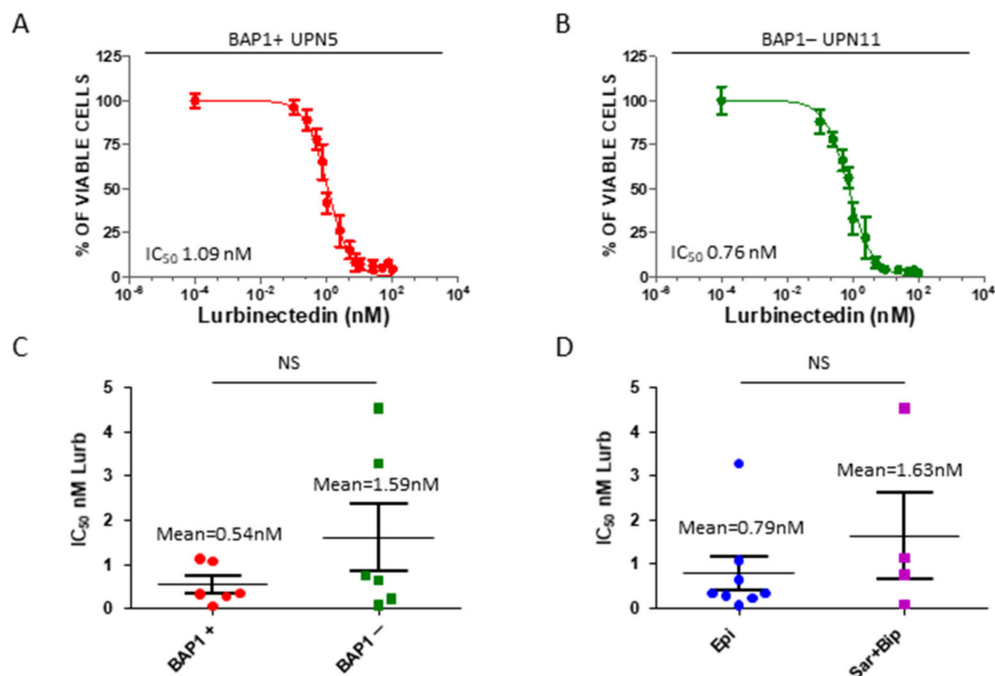


Figure 2. Patient-derived MPM cell lines sensitivity to lurbinectedin. (A,B) Representative dose-response curves and corresponding IC₅₀ values of the two indicated MPM cell lines treated with lurbinectedin (0.1 nM–100 nM) for 72 h. (C) Dot plot of IC₅₀ values measured in lurbinectedin-treated MPM cell lines positive or negative for BAP1 expression. ^{NS} $p > 0.05$. (D) Dot plot of IC₅₀ values measured in lurbinectedin-treated MPM cell lines grouped according to the histological subtype. ^{NS} $p > 0.05$.

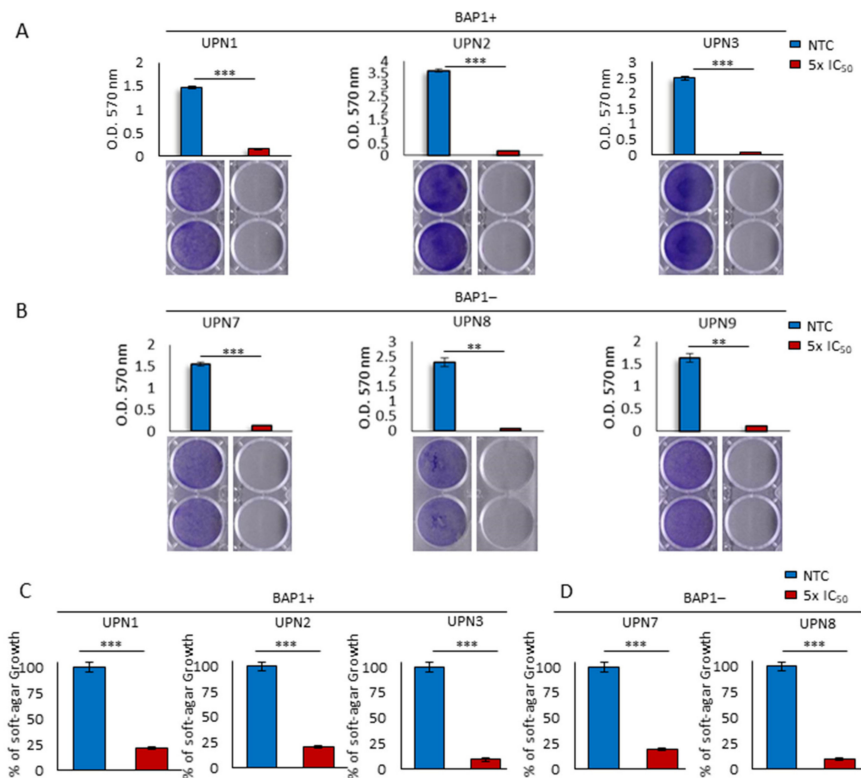


Figure 3. Lurbinectedin impairs long-term proliferation and anchorage-independent growth of MPM cell lines. (A,B) Representative pictures (lower panels) and quantification (upper panels) of crystal violet staining performed on the indicated MPM cell lines treated or not with lurbinectedin (5-fold the IC₅₀) for 10 days. Data are expressed as means ± SEM; ** *p* < 0.01; *** *p* < 0.001. (C,D) Soft agar growth assay quantification of the indicated MPM cell lines treated or not with lurbinectedin (5-fold the IC₅₀) for 20 days. The number of colonies obtained from untreated cells was set at 100%. Data are expressed as means ± SEM; *** *p* < 0.001.

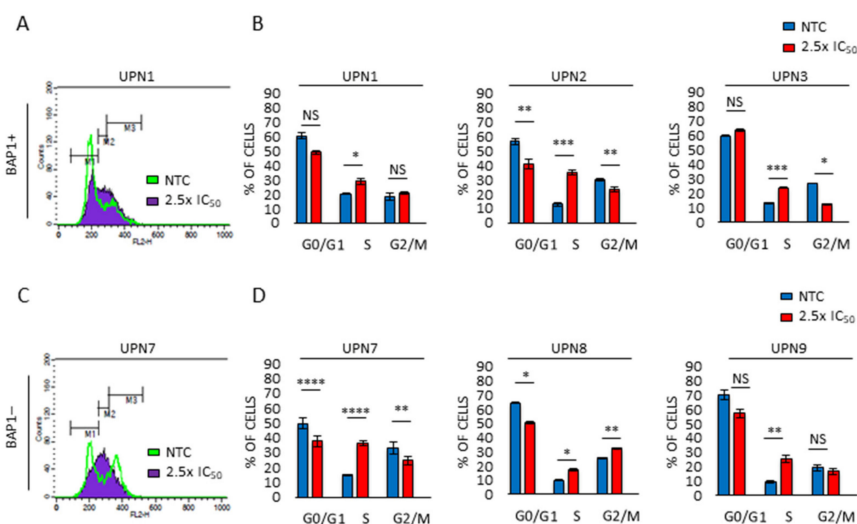


Figure 4. Lurbinectedin effects on cell cycle distribution. (A,C) Representative flow cytometry histogram showing the cell cycle distribution of the indicated MPM cell lines, treated (purple) or not (green) with lurbinectedin (2.5-fold the IC₅₀) for 24 h. (B,D) Histograms displaying cell number percentage in each cell cycle phase (G0/G1, S and G2/M) of the indicated MPM cell lines, treated or not with lurbinectedin (2.5-fold the IC₅₀) for 24 h. Data are expressed as means ± SEM; NS *p* > 0.05; * *p* < 0.05; ** *p* < 0.01; *** *p* < 0.001; **** *p* < 0.0001.

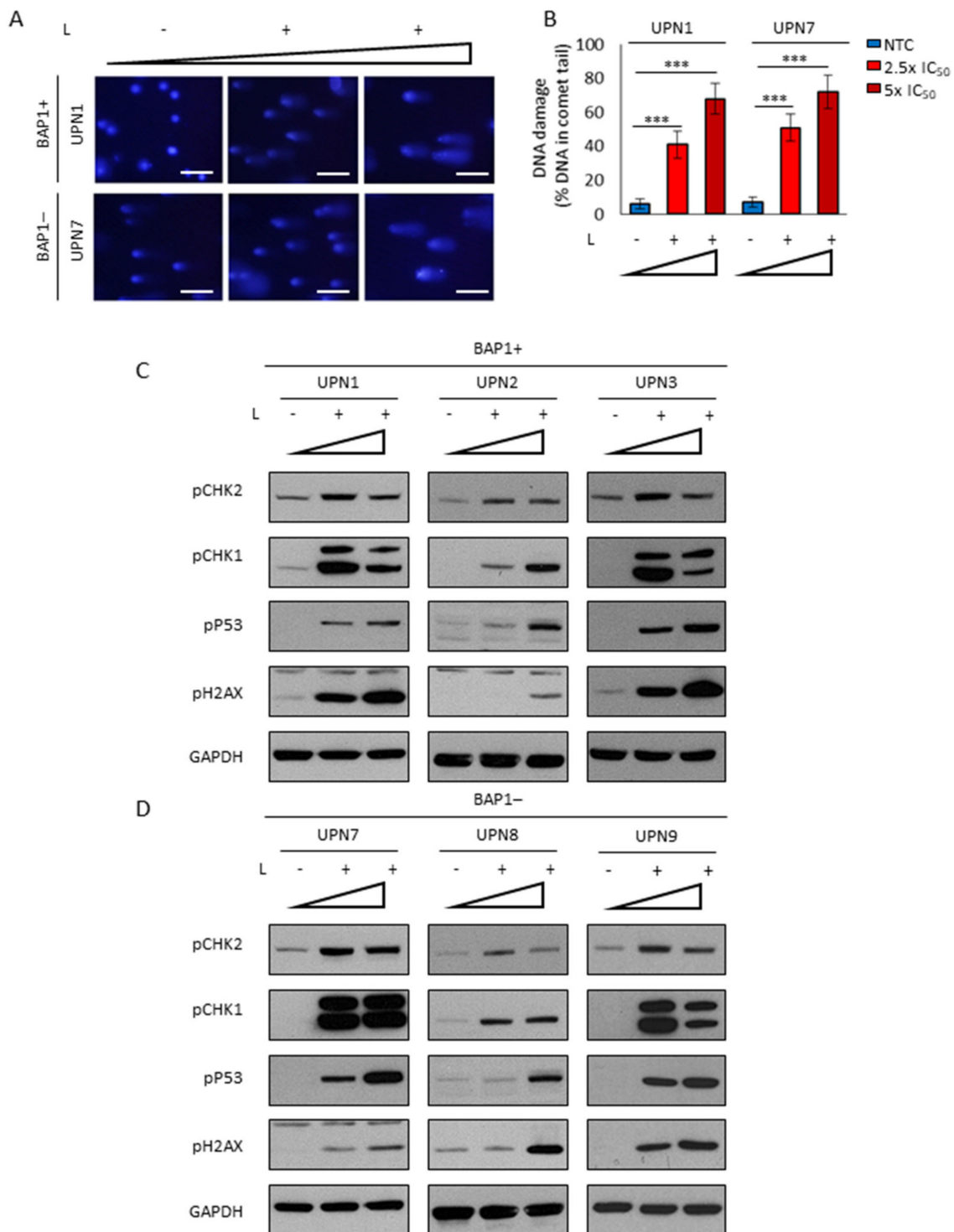


Figure 5. Lurbinectedin actively induces DNA damage response in MPM cell lines. (A) Representative Comet assay images of the indicated BAP1+ and BAP1- MPM cell lines treated or not with increasing lurbinectedin (L) concentrations (2.5-fold and 5-fold the IC₅₀) for 24h (scale bar = 5 μm). (B) Histograms showing Comet assay data quantitation by CometScore software. Bars represent a percentage of total DNA in the tail. Data are expressed as means ± SEM; *** *p* < 0.001. (C,D) Western blot analysis for the indicated proteins in BAP1+ and BAP1- MPM cell lines treated or not with increasing lurbinectedin (L) concentrations (2.5-fold and 5-fold the IC₅₀) for 24 h. GAPDH was used as a loading control.

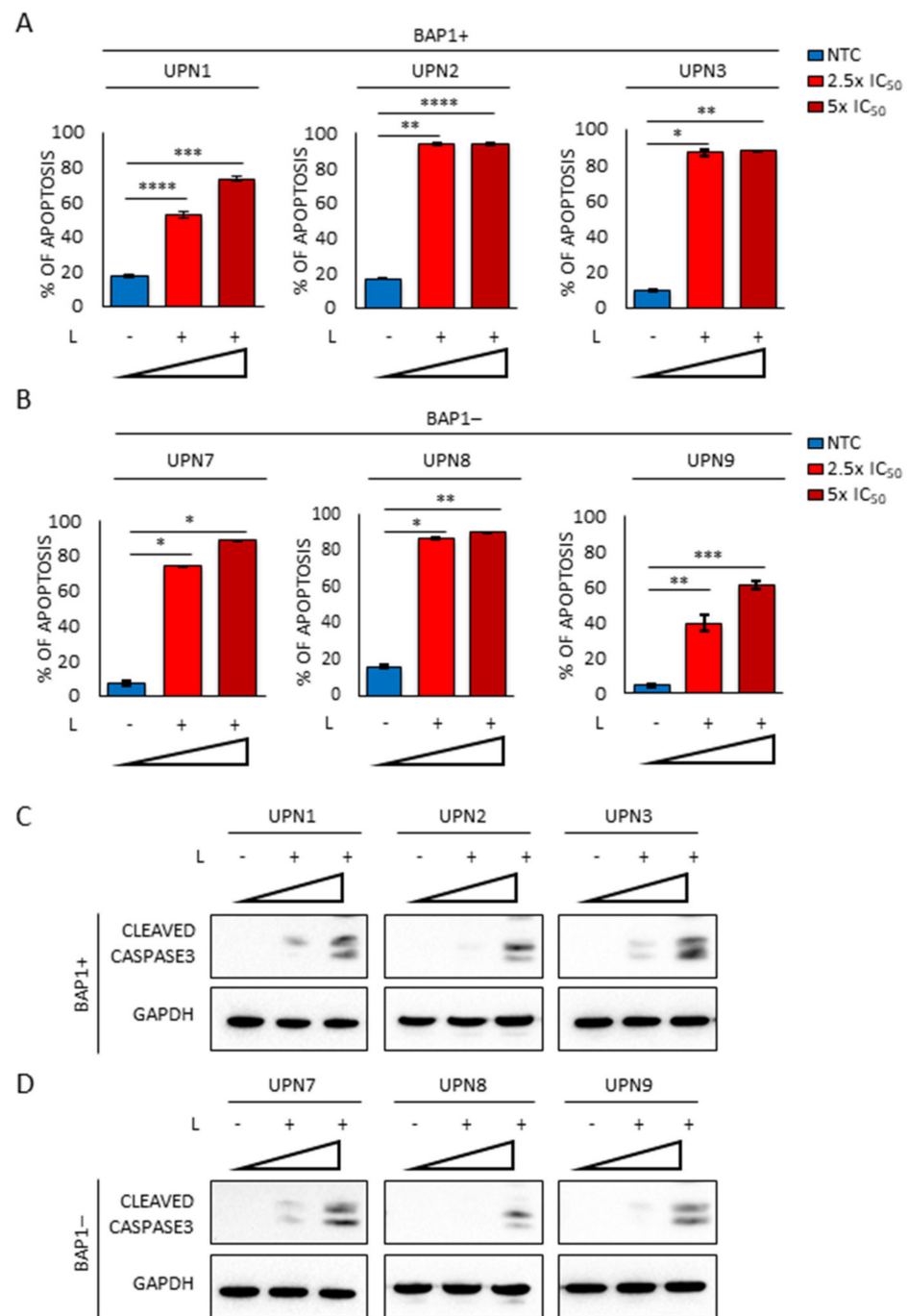


Figure 6. Lurbinectedin treatment strongly induces apoptosis in MPM cell lines. (A,B) Histograms representing the percentage of apoptotic MPM cells treated or not with increasing lurbinectedin (L) concentrations (2.5-fold and 5-fold the IC₅₀) for 72 h. The apoptotic rate was measured by TMRM assay. Data are expressed as means \pm SEM; * $p < 0.05$; ** $p < 0.01$; *** $p < 0.001$, **** $p < 0.0001$. (C,D) Western blot analysis of cleaved caspase 3 in MPM cell lines treated or not with increasing lurbinectedin (L) concentrations (2.5-fold and 5-fold the IC₅₀) for 24 h. GAPDH was used as a loading control.

3. Discussion

Malignant Pleural Mesothelioma (MPM) is an aggressive tumor marginally impacted by standard chemotherapy regimens. Moreover, the lack of effective molecular therapies as well as the immune-evasive tumor microenvironment makes the treatment of MPM particularly challenging [5–10,42]. Because MPM currently lacks peculiar oncogenic drivers,

we have explored the potential therapeutic efficacy of lurbinectedin, an alkylating agent which recently received FDA-conditional approval for the treatment of metastatic small cell lung cancer patients relapsing after chemotherapy [36].

We investigated the antitumor activity of lurbinectedin in a panel of 12 recently established primary MPM cell cultures. Our panel included all three MPM histotypes as well as cultures BAP1 positive and negative. Thus, although limited in terms of absolute number of cell lines, this panel is potentially representative of the different MPM phenotypes. Interestingly, we initially observed that lurbinectedin was effective at nanomolar concentrations and, as reported for other agents, its efficacy was independent of the BAP1 status. These data are particularly encouraging, although we are aware that freshly stabilized cultures could be potentially more sensitive to cytotoxic agents than what is usually observed at the clinical level. It is worthy of note, however, that three patients (UPN6, UPN10, UPN12) subsequently received trabectedin, a previous generation drug binding the minor groove of DNA, as second-line treatment. They did not show a superior clinical benefit compared to patients undergoing other treatments, indicating a limited efficacy of trabectedin. Interestingly, the MPM cells derived from these three patients had the highest IC₅₀ to lurbinectedin. These data may suggest that the response obtained in our stabilized cultures is a good surrogate of the potential effect of drugs binding the DNA minor groove and targeting the DNA repair observed in vivo.

Our experiments revealed that, as a consequence of the intrinsic ability of lurbinectedin to bind the minor groove of DNA, the drug interferes with the cell cycle, delaying progression through the S-phase. Interestingly, MPM cells immediately responded to genotoxic stress as demonstrated by the phosphorylation of H2AX, an early marker of the cellular response triggered by DNA double-strand breaks. Moreover, we observed the activation of Chk1 and Chk2 as a direct consequence of the stalled replication induced by DNA damage, responsible for the accumulation of MPM cells in the S-phase of the cell cycle. Finally, in our setting, p53 stabilization was not associated with DNA repair but invariably resulted in a massive apoptotic response, as revealed by cleaved caspase 3 activity and irreversible DNA fragmentation detected by Comet assay.

Notably, the efficacy of lurbinectedin against MPM was maintained also upon long-term treatment, as assessed by both crystal violet viability and anchorage-independent growth assays, providing further evidence of its anticancer potential.

As a consequence of DNA damage, replication arrest, and induction of apoptosis, we propose that lurbinectedin impairs the tumorigenic potential of MPM cells, and our results provide support to the clinical data recently reported in a multicentric phase II trial in second- or third-line palliative therapy [37]. Speculatively, considering the high anti-proliferative effect, if the results of the present study will be confirmed in MPM PDXs, lurbinectedin could be potentially investigated in the front line setting, for instance for a short pre-operative treatment in the early stages of MPM. Indeed, the reduction of anchorage-independent growth ability suggests lurbinectedin as a potential cytoreductive agent that, if proven in animal models and at the clinical level, will allow more conservative/less invasive surgery. Finally, the efficacy in all histotypes, independently from the BAP1 status, confers to lurbinectedin a strong advantage compared to other drugs currently used in MPM treatment, since its use could be potentially considered for all patients.

4. Materials and Methods

4.1. Reagents and Chemicals

Cell culture plasticware was obtained from Falcon (Glendale, AZ, USA), Biofil (Indore, India), and Costar (Washington, DC, USA). Lurbinectedin (PM01183) was kindly provided by PharmaMar (Madrid, Spain).

4.2. Cells

Primary MPM cells were obtained from biopsies during explorative thoracoscopy or pleurectomy, performed at the Thoracic Surgery Division of AOU Città della Salute e

della Scienza, Torino, Italy; AOU San Luigi Gonzaga, Orbassano, Italy, and AO of Alessandria, Biological Bank of Mesothelioma, Alessandria, Italy. Samples were anonymized by assigning an unknown patient number (UPN). Histological features of the original tumors and clinical features, including the first- and second-line treatment and the overall survival, of the corresponding patients are reported in Table S1. Samples were minced in 1 mm³-pieces, enzymatically digested for 1 h at 37 °C with 0.2 mg/mL hyaluronidase and 1 mg/mL collagenase [5], centrifuged at 1200× *g* for 5 min and seeded at 1 × 10⁶ cells/mL density in DMEM advanced/F12 (Gibco, Dublin, Ireland) until passage #5, when cultures were shifted to DMEM/F12 nutrient mixture medium (Sigma, Saint Louis, MO, USA). All media were supplemented with 10% heat-inactivated fetal bovine serum (FBS) (Sigma), 1% L-glutamine, 1% penicillin/streptomycin. Cells reached a stabilization (i.e., rate of cell subculture ≤1/week) in 2 to 7 months. UPN#3, UPN#4, UPN#5, UPN#6, UPN#10, UPN#11, UPN #12 were directly put in culture. UPN#1, UPN#2, UPN#7, UPN#8, UPN#9 were established from patient-derived xenografts. All cell lines were cultured in a humidified incubator at 37 °C in 5% CO₂ and routinely checked for *Mycoplasma* spp. contamination.

4.3. Patient-Derived Xenograft Generation

MPM patient-derived xenografts (PDXs) models were established from diagnostic tissue samples obtained at videothoracoscopy or during surgical pleurectomy. Each sample was implanted in the left or right side of the dorsal region of female NOD scid gamma (NSG) mice. A small piece of tumor was implanted subcutaneously and the wound was then stitched by surgical glue (Vetbond, Alcyon Italia, Cherasco, Italy). The tumor growth was monitored until the mass reached 2000 mm³. Then the animal was sacrificed by cervical dislocation, after anesthesia. The tumor area was shaved and disinfected with alcohol and the skin around the tumor was cut off. The tumor was divided into smaller pieces for re-implanting and collecting materials for further investigations. In the present work, the PDX platform was used as a tool to generate primary MPM cell cultures, stabilized in a shorter period (i.e., 2–3 months) than cells obtained directly from surgical procedures and used for pharmacological screening. To this aim, 0.2 g of tumors excised from the P1 generation of mice were digested to obtain a single-cell suspension [5] and put in culture as described in paragraph 4.2.

4.4. Immunohistochemical Analysis

The mesothelial features of cultures were confirmed by immunohistochemical (IHC) staining carried out on cells at passage 1. Specifically, cells were centrifuged at 1200× *g* for 5 min, fixed overnight in 4% *v/v* formalin at 4 °C, and then paraffin-embedded. The following antibodies were used: BAP-1 (Santa-Cruz Biotechnology, Santa Cruz, CA, USA, sc-28383, 1:100); Pan-cytokeratin AE1/AE3 (Dako, Agilent, Santa Clara, CA, USA, GA053, 1:500); Wilms Tumor-1 antigen (WT1) cl.6FH2 (Thermo Fisher Scientific, Waltham, MA, USA, MA1-46028, 1:10); Calretinin (Thermo Fisher Scientific, RB-9002-R7, 1:100). Mesothelial origin was confirmed if positivity for at least one between calretinin and WT1 was detected, as well as in the case of positivity for pancytokeratin. The histological features are reported in Table 1.

4.5. IC₅₀ Calculation

Cells were seeded in 96-well plates at a density of 2 × 10³/well and serially diluted lurbinedectin (0.01 nM–100 nM) was added to the medium. After 72 h of treatment, IC₅₀ was evaluated with CellTiter-Glo (Promega) according to the manufacturer's instructions, using a Cytation 3 Imaging Reader (Bio-Tek Instruments, Winooski, VT, USA).

4.6. Crystal Violet Assay

For long-term proliferation, cells were seeded at a density of 4 × 10³/well in 12-well plates and treated with the indicated concentrations of lurbinedectin for 10 days. Subsequently, cells were fixed and stained with 5% *w/v* crystal violet solution in 66% *v/v*

methanol and washed. Crystal violet was eluted by adding 10% acetic acid into each well. Quantification was performed by measuring the absorbance (570 nm) with Cytation 3 Imaging Reader (Bio-Tek Instruments).

4.7. Soft-Agar Assay

For anchorage-independent cell growth assay, cells were suspended in 0.45% type VII low-melting agarose in medium supplemented with 10% FBS at 1×10^5 cells/well, plated on a layer of 0.9% agarose in 10% FBS medium in 6-well plates, and cultured for 20–30 days with the indicated concentrations of lurbinedectin.

4.8. Cell Cycle Analysis

Cells were plated at a density of 1.2×10^5 /well in 6-well plates and treated with the indicated concentrations of lurbinedectin for 24 h. Subsequently, cells were washed in PBS, treated with RNase (167 $\mu\text{g}/\text{mL}$), and stained for 15 min at RT with propidium iodide (33 $\mu\text{g}/\text{mL}$). The cell-cycle distribution in G0/G1, S, and G2/M phases was analyzed by FACSCalibur flow cytometer (Becton Dickinson, Franklin Lanes, NJ, USA) and calculated using the CellQuest program (Becton Dickinson).

4.9. Apoptosis Detection Assay

MPM cells were plated at a density of 1.2×10^5 /well in 6-well plates and treated with the indicated concentrations of lurbinedectin for 72 h. Subsequently, floating and adherent cells were washed with PBS and stained with tetramethylrhodamine methylester perchlorate (TMRM) (200 nM) for 15 min at RT. The percentage of apoptosis was measured by FACSCalibur flow cytometer (Becton Dickinson) and calculated using the CellQuest program (Becton Dickinson).

4.10. Comet Assay

DNA damage was assessed by Single Cell Gel Electrophoresis assay (Comet assay) [43]. At least 100 nuclei were counted in each condition. The percentage of DNA in the tail was quantified using the CometScore software (TriTek Corp., Sumerduck, VA, USA).

4.11. Western Blot Analysis

Cells were washed with ice-cold PBS and incubated for 20 min on ice in 0.1% Triton X-100 lysis buffer (20 mM Tris HCl pH 7.4; 150 mM NaCl; 5 mM EDTA; 0.1% Triton X-100; 1 mM Phenylmethanesulfonyl fluoride; 10 mM NaF; 1 mM Na_3VO_4 , supplemented with protease inhibitor cocktail). Cells were then centrifuged at $14,000 \times g$ for 15 min at 4°C to remove any cellular debris. Protein lysates were subsequently quantified using DC protein assay (Bio-Rad), loaded in 4–12% NuPAGE Bis-Tris Protein Gels (Thermo Fisher Scientific) according to the manufacturer's instructions, and transferred onto Hybond ECL nitrocellulose membranes. Blocking was performed with 5% Nonfat dried milk (PanReac AppliChem, Darmstadt, Germany) for 45 min at RT. Membranes were then incubated O/N at 4°C with the following antibodies: BAP-1 (Santa Cruz Biotechnology, sc-28383); phospho(Ser345) Chk1 (Cell Signaling, Danvers, MA, USA, 2348); phospho(Thr68) Chk2 (Cell Signaling, 2197); phospho(Ser15) p53 (Cell Signaling, 9286); GAPDH (Cell Signaling, 5174); cleaved Caspase3 (Cell Signaling, 9661); phospho(Ser139)-Histone H2A.X (Cell Signaling, 9718); rabbit IgG, HRP-linked (Cell Signaling, 7074); mouse IgG, HRP-linked (Cell Signaling, 7076). Proteins were detected with horseradish peroxidase-conjugated secondary antibodies and Pierce™ ECL Western Blotting Substrate.

4.12. Image Processing

Image acquisition was performed with Leica dmire2 microscope and with Olympus BX51. Images were processed with the ImageJ software package (<https://imagej.nih.gov/ij/> accessed on 16 April 2021).

4.13. Statistical Analysis

All values were expressed as mean \pm SEM and derived from at least two independent experiments. Statistical analyses were performed using Microsoft Excel and GraphPad Prism 5. Graphs were generated using Microsoft Excel and GraphPad Prism. Two-tailed Student's t-test was used to evaluate statistical significance: ^{NS} $p > 0.05$; * $p < 0.05$; ** $p < 0.01$; *** $p < 0.001$; **** $p < 0.0001$.

5. Conclusions

Overall, our work proves the efficacy of lurbinectedin at nanomolar concentration against primary MPM cells. Although obtained in a relatively small cohort, that however is representative of the different MPM phenotypes, our results are particularly encouraging and put the basis for investigating lurbinectedin in different therapeutic settings of MPM.

Supplementary Materials: The following are available online at <https://www.mdpi.com/article/10.3390/cancers13102332/s1>, Figure S1: Lurbinectedin effects on cell cycle distribution, Figure S2: Lurbinectedin treatment strongly impairs cell viability in MPM cell lines, Table S1: Histological features of the original tumors and clinical features of the corresponding patients.

Author Contributions: Conceptualization, C.R., R.T., G.V.S., F.P., P.B., and D.P.A.; methodology, F.P., D.P.A., M.F.L., D.M., L.R., F.N., M.G.P., A.P., F.D.N., C.G., F.B., V.C., F.G., A.S., F.L., R.L., P.A., and S.N.; writing—review and editing C.R., R.T., G.V.S., and P.B.; supervision, C.R., R.T., P.B., and G.V.S. All authors have read and agreed to the published version of the manuscript.

Funding: The research plan has received funding from AIRC under IG 2019—ID. 23760 project to G.V.S and IG 2019 ID. 21408 project to C.R. EX60% Funding 2019 to P.B.; ERA-Net Transcan-2-JTC 2017 (TOPMESO to F.B.). PharmaMar kindly provided the drug for the study without any influence on the conduction of the experiments.

Institutional Review Board Statement: The study was conducted according to the guidelines of the Declaration of Helsinki and approved by the Ethics Committee of San Luigi Hospital (#126/2016) and the Biological Bank of Mesothelioma, S. Antonio e Biagio Hospital, Alessandria, Italy (#9/11/2011). All animal procedures were performed in accordance with the national, institutional, and international law, policies, and guidelines (NIH guide for the Care and Use of Laboratory Animals -2011 edition-; European Economic Community (EEC) Council Directive 2010/63/UE; Italian Governing Law D. lg 26/2014). The animal study was approved by the Ethical Committee of the University of Turin and by the Italian Ministry of Health (400/2017-PR).

Informed Consent Statement: Informed consent was obtained from all subjects involved in the study.

Data Availability Statement: The data presented in this study are available in this article (and Supplementary Materials).

Acknowledgments: We are grateful to all patients and their families who participated in the study.

Conflicts of Interest: G.V.S. received honoraria from AstraZeneca, Eli Lilly, MSD, Pfizer, Roche, Johnson & Johnson, Takeda; consulting or advisory role for Eli Lilly, Beigene, and AstraZeneca, received institutional research funding from Eli Lilly and MSD and received travel, accommodations from Bayer. The Riganti and Taulli laboratories have received research support from PharmaMar. The other authors declare no conflict of interest. The funders had no role in the design of the study; in the collection, analyses, or interpretation of data; in the writing of the manuscript, or in the decision to publish the results.

References

1. Peto, J.; Decarli, A.; Vecchia, C.L.; Levi, F.; Negri, E. The European Mesothelioma Epidemic. *Br. J. Cancer* **1999**, *79*, 666–672. [[CrossRef](#)]
2. Chen, T.; Sun, X.-M.; Wu, L. High Time for Complete Ban on Asbestos Use in Developing Countries. *JAMA Oncol.* **2019**, *5*, 779–780. [[CrossRef](#)] [[PubMed](#)]
3. Yap, T.A.; Aerts, J.G.; Popat, S.; Fennell, D.A. Novel Insights into Mesothelioma Biology and Implications for Therapy. *Nat. Rev. Cancer* **2017**, *17*, 475–488. [[CrossRef](#)] [[PubMed](#)]

4. Kojima, M.; Kajino, K.; Momose, S.; Wali, N.; Hlaing, M.T.; Han, B.; Yue, L.; Abe, M.; Fujii, T.; Ikeda, K.; et al. Possible Reversibility between Epithelioid and Sarcomatoid Types of Mesothelioma Is Independent of ERC/Mesothelin Expression. *Respir. Res.* **2020**, *21*, 187. [[CrossRef](#)]
5. Salaroglio, I.C.; Kopecka, J.; Napoli, F.; Pradotto, M.; Maletta, F.; Costardi, L.; Gagliasso, M.; Milosevic, V.; Ananthanarayanan, P.; Bironzo, P.; et al. Potential Diagnostic and Prognostic Role of Microenvironment in Malignant Pleural Mesothelioma. *J. Thorac. Oncol.* **2019**, *14*, 1458–1471. [[CrossRef](#)] [[PubMed](#)]
6. Hegmans, J.P.J.; Hemmes, A.; Hammad, H.; Boon, L.; Hoogsteden, H.C.; Lambrecht, B.N. Mesothelioma Environment Comprises Cytokines and T-Regulatory Cells That Suppress Immune Responses. *Eur. Respir. J.* **2006**, *27*, 1086–1095. [[CrossRef](#)] [[PubMed](#)]
7. Veltman, J.D.; Lambers, M.E.H.; van Nimwegen, M.; Hendriks, R.W.; Hoogsteden, H.C.; Aerts, J.G.J.V.; Hegmans, J.P.J. COX-2 Inhibition Improves Immunotherapy and Is Associated with Decreased Numbers of Myeloid-Derived Suppressor Cells in Mesothelioma. Celecoxib Influences MDSC Function. *BMC Cancer* **2010**, *10*, 464. [[CrossRef](#)] [[PubMed](#)]
8. Ujii, H.; Kadota, K.; Nitadori, J.; Aerts, J.G.; Woo, K.M.; Sima, C.S.; Travis, W.D.; Jones, D.R.; Krug, L.M.; Adusumilli, P.S. The Tumoral and Stromal Immune Microenvironment in Malignant Pleural Mesothelioma: A Comprehensive Analysis Reveals Prognostic Immune Markers. *Oncoimmunology* **2015**, *4*, e1009285. [[CrossRef](#)]
9. Chu, G.J.; van Zandwijk, N.; Rasko, J.E.J. The Immune Microenvironment in Mesothelioma: Mechanisms of Resistance to Immunotherapy. *Front. Oncol.* **2019**, *9*, 1366. [[CrossRef](#)]
10. Riganti, C.; Lingua, M.F.; Salaroglio, I.C.; Falcomatà, C.; Righi, L.; Morena, D.; Picca, F.; Oddo, D.; Kopecka, J.; Pradotto, M.; et al. Bromodomain Inhibition Exerts Its Therapeutic Potential in Malignant Pleural Mesothelioma by Promoting Immunogenic Cell Death and Changing the Tumor Immune-Environment. *Oncoimmunology* **2018**, *7*, e1398874. [[CrossRef](#)]
11. Cinausero, M.; Rihawi, K.; Sperandi, F.; Melotti, B.; Ardizzoni, A. Chemotherapy Treatment in Malignant Pleural Mesothelioma: A Difficult History. *J. Thorac. Dis.* **2018**, *10*, S304–S310. [[CrossRef](#)]
12. Baas, P.; Scherpereel, A.; Nowak, A.K.; Fujimoto, N.; Peters, S.; Tsao, A.S.; Mansfield, A.S.; Papat, S.; Jahan, T.; Antonia, S.; et al. First-Line Nivolumab plus Ipilimumab in Unresectable Malignant Pleural Mesothelioma (CheckMate 743): A Multicentre, Randomised, Open-Label, Phase 3 Trial. *Lancet* **2021**, *397*, 375–386. [[CrossRef](#)]
13. Nicolini, F.; Bocchini, M.; Bronte, G.; Delmonte, A.; Guidoboni, M.; Crinò, L.; Mazza, M. Malignant Pleural Mesothelioma: State-of-the-Art on Current Therapies and Promises for the Future. *Front. Oncol.* **2019**, *9*, 1519. [[CrossRef](#)]
14. Cantini, L.; Hassan, R.; Serman, D.H.; Aerts, J.G.J.V. Emerging Treatments for Malignant Pleural Mesothelioma: Where Are We Heading? *Front. Oncol.* **2020**, *10*, 343. [[CrossRef](#)]
15. Hmeljak, J.; Sanchez-Vega, F.; Hoadley, K.A.; Shih, J.; Stewart, C.; Heiman, D.; Tarpey, P.; Danilova, L.; Drill, E.; Gibb, E.A.; et al. Integrative Molecular Characterization of Malignant Pleural Mesothelioma. *Cancer Discov.* **2018**, *8*, 1548–1565. [[CrossRef](#)]
16. Bueno, R.; Stawiski, E.W.; Goldstein, L.D.; Durinck, S.; de Rienzo, A.; Modrusan, Z.; Gnad, F.; Nguyen, T.T.; Jaiswal, B.S.; Chiriac, L.R.; et al. Comprehensive Genomic Analysis of Malignant Pleural Mesothelioma Identifies Recurrent Mutations, Gene Fusions and Splicing Alterations. *Nat. Genet.* **2016**, *48*, 407–416. [[CrossRef](#)] [[PubMed](#)]
17. Guo, G.; Chmielecki, J.; Goparaju, C.; Heguy, A.; Dolgalev, I.; Carbone, M.; Seepo, S.; Meyerson, M.; Pass, H.I. Whole-Exome Sequencing Reveals Frequent Genetic Alterations in BAP1, NF2, CDKN2A, and CUL1 in Malignant Pleural Mesothelioma. *Cancer Res.* **2015**, *75*, 264–269. [[CrossRef](#)] [[PubMed](#)]
18. Patil, N.S.; Righi, L.; Koeppen, H.; Zou, W.; Izzo, S.; Grosso, F.; Libener, R.; Loiacono, M.; Monica, V.; Buttiglieri, C.; et al. Molecular and Histopathological Characterization of the Tumor Immune Microenvironment in Advanced Stage of Malignant Pleural Mesothelioma. *J. Thorac. Oncol.* **2018**, *13*, 124–133. [[CrossRef](#)]
19. Nasu, M.; Emi, M.; Pastorino, S.; Tanji, M.; Powers, A.; Luk, H.; Baumann, F.; Zhang, Y.-A.; Gazdar, A.; Kanodia, S.; et al. High Incidence of Somatic BAP1 Alterations in Sporadic Malignant Mesothelioma. *J. Thorac. Oncol.* **2015**, *10*, 565–576. [[CrossRef](#)]
20. Bott, M.; Brevet, M.; Taylor, B.S.; Shimizu, S.; Ito, T.; Wang, L.; Creaney, J.; Lake, R.A.; Zakowski, M.F.; Reva, B.; et al. The Nuclear Deubiquitinase BAP1 Is Commonly Inactivated by Somatic Mutations and 3p21.1 Losses in Malignant Pleural Mesothelioma. *Nat. Genet.* **2011**, *43*, 668–672. [[CrossRef](#)]
21. Carbone, M.; Flores, E.G.; Emi, M.; Johnson, T.A.; Tsunoda, T.; Behner, D.; Hoffman, H.; Hesdorffer, M.; Nasu, M.; Napolitano, A.; et al. Combined Genetic and Genealogic Studies Uncover a Large BAP1 Cancer Syndrome Kindred Tracing Back Nine Generations to a Common Ancestor from the 1700s. *PLoS Genet.* **2015**, *11*, e1005633. [[CrossRef](#)] [[PubMed](#)]
22. Testa, J.R.; Cheung, M.; Pei, J.; Below, J.E.; Tan, Y.; Sementino, E.; Cox, N.J.; Dogan, A.U.; Pass, H.I.; Trusa, S.; et al. Germline BAP1 Mutations Predispose to Malignant Mesothelioma. *Nat. Genet.* **2011**, *43*, 1022–1025. [[CrossRef](#)] [[PubMed](#)]
23. Carbone, M.; Harbour, J.W.; Brugarolas, J.; Bononi, A.; Pagano, I.; Dey, A.; Krausz, T.; Pass, H.I.; Yang, H.; Gaudino, G. Biological Mechanisms and Clinical Significance of BAP1 Mutations in Human Cancer. *Cancer Discov.* **2020**, *10*, 1103–1120. [[CrossRef](#)] [[PubMed](#)]
24. Lee, H.-S.; Lee, S.-A.; Hur, S.-K.; Seo, J.-W.; Kwon, J. Stabilization and Targeting of INO80 to Replication Forks by BAP1 during Normal DNA Synthesis. *Nat. Commun.* **2014**, *5*, 5128. [[CrossRef](#)]
25. Lee, H.-S.; Seo, H.-R.; Lee, S.-A.; Choi, S.; Kang, D.; Kwon, J. BAP1 Promotes Stalled Fork Restart and Cell Survival via INO80 in Response to Replication Stress. *Biochem. J.* **2019**, *476*, 3053–3066. [[CrossRef](#)]
26. Yu, H.; Pak, H.; Hammond-Martel, I.; Ghram, M.; Rodrigue, A.; Daou, S.; Barbour, H.; Corbeil, L.; Hébert, J.; Drobetsky, E.; et al. Tumor Suppressor and Deubiquitinase BAP1 Promotes DNA Double-Strand Break Repair. *Proc. Natl. Acad. Sci. USA* **2014**, *111*, 285–290. [[CrossRef](#)]

27. Nishikawa, H.; Wu, W.; Koike, A.; Kojima, R.; Gomi, H.; Fukuda, M.; Ohta, T. BRCA1-Associated Protein 1 Interferes with BRCA1/BARD1 RING Heterodimer Activity. *Cancer Res.* **2009**, *69*, 111–119. [[CrossRef](#)]
28. Santamaría Nuñez, G.; Robles, C.M.G.; Giraudon, C.; Martínez-Leal, J.F.; Compe, E.; Coin, F.; Aviles, P.; Galmarini, C.M.; Egly, J.-M. Lurbinectedin Specifically Triggers the Degradation of Phosphorylated RNA Polymerase II and the Formation of DNA Breaks in Cancer Cells. *Mol. Cancer Ther.* **2016**, *15*, 2399–2412. [[CrossRef](#)]
29. Poveda, A.; Del Campo, J.M.; Ray-Coquard, I.; Alexandre, J.; Provansal, M.; Guerra Alía, E.M.; Casado, A.; Gonzalez-Martin, A.; Fernández, C.; Rodríguez, I.; et al. Phase II Randomized Study of PM01183 versus Topotecan in Patients with Platinum-Resistant/Refractory Advanced Ovarian Cancer. *Ann. Oncol.* **2017**, *28*, 1280–1287. [[CrossRef](#)]
30. Vidal, A.; Muñoz, C.; Guillén, M.-J.; Moretó, J.; Puertas, S.; Martínez-Iniesta, M.; Figueras, A.; Padullés, L.; García-Rodríguez, F.J.; Berdiel-Acer, M.; et al. Lurbinectedin (PM01183), a New DNA Minor Groove Binder, Inhibits Growth of Orthotopic Primary Graft of Cisplatin-Resistant Epithelial Ovarian Cancer. *Clin. Cancer Res.* **2012**, *18*, 5399–5411. [[CrossRef](#)]
31. Leal, J.F.M.; Martínez-Díez, M.; García-Hernández, V.; Moneo, V.; Domingo, A.; Bueren-Calabuig, J.A.; Negri, A.; Gago, F.; Guillén-Navarro, M.J.; Avilés, P.; et al. PM01183, a New DNA Minor Groove Covalent Binder with Potent in Vitro and in Vivo Anti-Tumour Activity. *Br. J. Pharmacol.* **2010**, *161*, 1099–1110. [[CrossRef](#)] [[PubMed](#)]
32. Cruz, C.; Llop-Guevara, A.; Garber, J.E.; Arun, B.K.; Pérez Fidalgo, J.A.; Lluch, A.; Telli, M.L.; Fernández, C.; Kahatt, C.; Galmarini, C.M.; et al. Multicenter Phase II Study of Lurbinectedin in BRCA-Mutated and Unselected Metastatic Advanced Breast Cancer and Biomarker Assessment Substudy. *J. Clin. Oncol.* **2018**, *36*, 3134–3143. [[CrossRef](#)] [[PubMed](#)]
33. Benton, C.B.; Chien, K.S.; Tefferi, A.; Rodríguez, J.; Ravandi, F.; Daver, N.; Jabbour, E.; Jain, N.; Alvarado, Y.; Kwari, M.; et al. Safety and Tolerability of Lurbinectedin (PM01183) in Patients with Acute Myeloid Leukemia and Myelodysplastic Syndrome. *Hematol. Oncol.* **2019**, *37*, 96–102. [[CrossRef](#)]
34. Cote, G.M.; Choy, E.; Chen, T.; Marino-Enriquez, A.; Morgan, J.; Merriam, P.; Thornton, K.; Wagner, A.J.; Nathenson, M.J.; Demetri, G.; et al. A Phase II Multi-Strata Study of Lurbinectedin as a Single Agent or in Combination with Conventional Chemotherapy in Metastatic and/or Unresectable Sarcomas. *Eur. J. Cancer* **2020**, *126*, 21–32. [[CrossRef](#)] [[PubMed](#)]
35. Calvo, E.; Moreno, V.; Flynn, M.; Holgado, E.; Olmedo, M.E.; Criado, M.L.; Kahatt, C.; Lopez-Vilariño, J.A.; Siguero, M.; Fernandez-Teruel, C.; et al. Antitumor Activity of Lurbinectedin (PM01183) and Doxorubicin in Relapsed Small-Cell Lung Cancer: Results from a Phase I Study. *Ann. Oncol. Off. J. Eur. Soc. Med. Oncol.* **2017**, *28*, 2559–2566. [[CrossRef](#)] [[PubMed](#)]
36. Singh, S.; Jaigirdar, A.A.; Mulkey, F.; Cheng, J.; Hamed, S.S.; Li, Y.; Liu, J.; Zhao, H.; Goheer, A.; Helms, W.S.; et al. FDA Approval Summary: Lurbinectedin for the Treatment of Metastatic Small Cell Lung Cancer. *Clin. Cancer Res.* **2020**, *27*, 2378–2382. [[CrossRef](#)]
37. Metaxas, Y.; Früh, M.; Eboulet, E.I.; Grosso, F.; Pless, M.; Zucali, P.A.; Ceresoli, G.L.; Mark, M.; Schneider, M.; Maconi, A.; et al. Lurbinectedin as Second- or Third-Line Palliative Therapy in Malignant Pleural Mesothelioma: An International, Multi-Centre, Single-Arm, Phase II Trial (SAKK 17/16). *Ann. Oncol.* **2020**, *31*, 495–500. [[CrossRef](#)]
38. Soares, D.G.; Machado, M.S.; Rocca, C.J.; Poindessous, V.; Ouaret, D.; Sarasin, A.; Galmarini, C.M.; Henriques, J.A.P.; Escargueil, A.E.; Larsen, A.K. Trabectedin and Its C Subunit Modified Analogue PM01183 Attenuate Nucleotide Excision Repair and Show Activity toward Platinum-Resistant Cells. *Mol. Cancer Ther.* **2011**, *10*, 1481–1489. [[CrossRef](#)]
39. Minchom, A.; Aversa, C.; Lopez, J. Dancing with the DNA Damage Response: Next-Generation Anti-Cancer Therapeutic Strategies. *Ther. Adv. Med. Oncol.* **2018**, *10*, 1758835918786658. [[CrossRef](#)]
40. Cho, Y.-J.; Liang, P. S-Phase-Coupled Apoptosis in Tumor Suppression. *Cell. Mol. Life Sci.* **2011**, *68*, 1883–1896. [[CrossRef](#)]
41. Lee, S.Y.; Russell, P. Brc1 Links Replication Stress Response and Centromere Function. *Cell Cycle* **2013**, *12*, 1665–1671. [[CrossRef](#)] [[PubMed](#)]
42. Guazzelli, A.; Meysami, P.; Bakker, E.; Bonanni, E.; Demonacos, C.; Krstic-Demonacos, M.; Mutti, L. What Can Independent Research for Mesothelioma Achieve to Treat This Orphan Disease? *Expert Opin. Investig. Drugs* **2019**, *28*, 719–732. [[CrossRef](#)] [[PubMed](#)]
43. Freyria, F.S.; Bonelli, B.; Tomatis, M.; Ghiazza, M.; Gazzano, E.; Ghigo, D.; Garrone, E.; Fubini, B. Hematite Nanoparticles Larger than 90 Nm Show No Sign of Toxicity in Terms of Lactate Dehydrogenase Release, Nitric Oxide Generation, Apoptosis, and Comet Assay in Murine Alveolar Macrophages and Human Lung Epithelial Cells. *Chem. Res. Toxicol.* **2012**, *25*, 850–861. [[CrossRef](#)] [[PubMed](#)]